

Low-Field Transport Model for Semiconducting Carbon Nanotubes

Gary Pennington, Akin Akturk, and Neil Goldsman

Department of Electrical and Computer Engineering, University of Maryland, College Park, MD 20742, USA

Email: {garyp,akturka,neil}@glue.umd.edu

Abstract – Transport models for carrier transport in a semiconducting carbon nanotube are presented. Results encompass tubes of varying diameter and chirality. The focus is on transport in response to a small, axially applied electric field.

Models for phonon-limited transport are developed whereby carriers scatter with stretching, twisting, and radial breathing acoustic phonons. The resulting mobility model agrees well with experiments, showing very large mobility ($>10^5$ cm²/Vs) at room temperature. Furthermore, the transport model predicts a mean free path in large diameter tubes very close to experimental results (700nm). Our model predicts that the mobility and the mean free path will increase with tube diameter and decrease with temperature when phonon scattering dominates. Nonparabolic corrections to the band structure are found to greatly impact transport modeling.

The transport regime dominated by scattering from localized charges is also considered. A low-field mobility model for carrier scattering with interface charge is presented. Results show mobility increasing rapidly with tube diameter and increasing slowly with temperature.

I. INTRODUCTION

Currently, there is immense interest in possible electronic applications for semiconducting carbon nanotubes. These include use as small and fast electronic devices, high mobility implants in conventional Si-based devices, chemical and biological sensors, and electron memory elements [1, 2]. The performance of these devices, determined by either the switching speed or sensitivity, is expected to improve as the carrier mobility increases. Recent experiments have shown encouraging results, indicating that the mobility is exceptionally large in very long semiconducting single-walled carbon nanotubes (SWCNTs) [1].

The focus of this work is the development of a model for the transport properties of semiconducting SWCNTs subject to a low applied electric field along the tube axis. Scattering mechanisms considered result

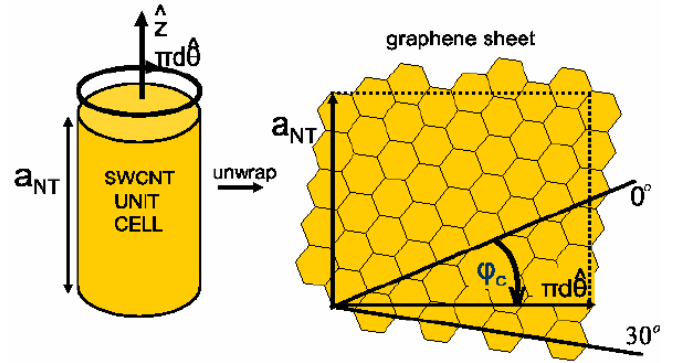


Figure 1: SWCNT lattice

from carrier interactions with phonons and localized external charges. Transport limited by phonon scattering is considered in section II. Coulombic scattering from localized charges may also be important in nanotube devices. In section III, a model for the mobility in the presence of a high density of charges near the nanotube surface is developed.

As shown in Fig. 1, the diameter (d) and chiral angle (ϕ_c) must be known in order to uniquely specify a given SWCNT. The electronic properties of a carbon nanotube will vary depending on d and ϕ_c . It is desirable to have transport models which can account for these variations and therefore universally describe transport in all semiconducting SWCNTs.

At low axial fields the carrier energies near the minimum of the lowest subband are of importance. The relevant energy-wavevector relation $E(k)$ can be described using a nonparabolic band shape:

$$\frac{\hbar^2 k^2}{2[m_e/11.37\tilde{d}]} = E(1 + \alpha E), \quad \alpha = 1/E_{gap} \propto d. \quad (1)$$

Here m_e is the electron mass, α is the nonparabolic factor, and the term in square brackets is the effective mass (m^*). To aid in the application of the transport models to different nanotubes, dimensionless expressions $\tilde{d} = d/1\text{nm}$ and $\tilde{T} = T/300\text{K}$ will be used for the tube diameter and lattice temperature respectively. The effective mass is inversely proportional to d while

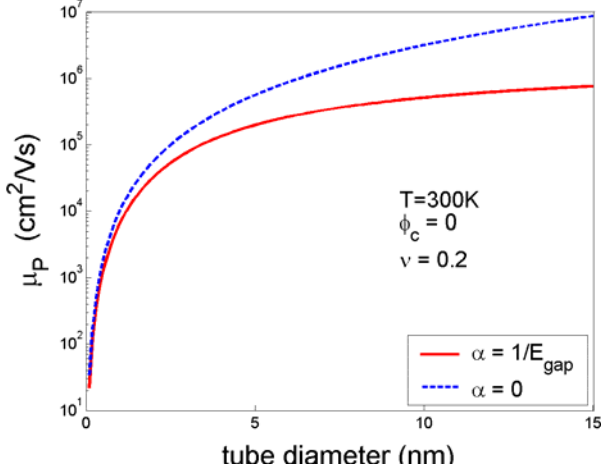


Figure 2: Low-field phonon scattering mobility vs. d

the nonparabolic factor is proportional to d . These dependences strongly influence the diameter dependence of other transport properties such as the mobility and the relaxation length. Note that at low energies, $E(k)$ only influences transport through m^* and α which are independent of chirality ϕ_c .

II. PHONON-LIMITED TRANSPORT

In this section a model for carrier transport dominated by phonon scattering is discussed. Previous work [3, 4] is now expanded to include all possible semiconducting SWCNTs and all relevant phonon modes. Theoretical results are developed for the semiclassical transport of carriers subject to scattering with stretching, twisting, and breathing acoustic phonon modes. Here a chirality dependence arises at low-fields since the acoustic phonon deformation potential D depends on ϕ_c . In accord with previous theoretical work, the deformation potential is independent of tube diameter [5, 6]. We use $D = 7F_c eV$ where the chirality factor is:

$$F_c = \left| (1 + \nu) \cos(3\phi_c) - i \frac{\mathcal{G}_L}{\mathcal{G}_T} \sin(3\phi_c) \right|. \quad (2)$$

Here the chirality factor depends on the Poisson ratio ν , the longitudinal ($\mathcal{G}_L=21\text{km/s}$) and transverse ($\mathcal{G}_T=15\text{km/s}$) sound velocities, and the chiral angle ϕ_c . The graphene value of $\nu=0.2$ is used for the SWCNT. The deformation potential above has been reduced from the theoretical result [5, 6] by a factor of $\sim 10\%$ in order to fit experimental data.

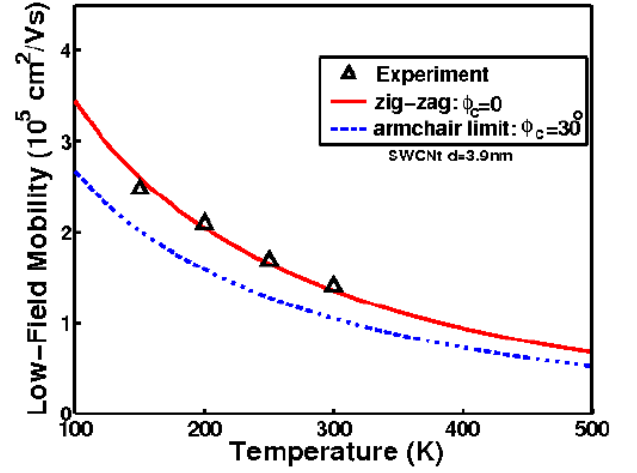


Figure 3: Phonon scattering mobility vs. T

By solving the ensemble averaged momentum balance relation, the low-field carrier mobility is found as:

$$\mu_p = 10^4 \frac{\text{cm}^2}{\text{Vs}} \cdot \frac{\tilde{d}^{5/2}}{F_c^2 \sqrt{\tilde{T}}} \left[\frac{1 + \frac{3}{4}\chi - \frac{21}{32}\chi^2}{1 + 2\chi + 30\chi^2} \right]. \quad (3)$$

Here $1 \times 10^4 \text{ cm}^2/\text{Vs}$ is the room temperature low-field mobility for a SWCNT with $F_c=1$, $d=1\text{nm}$, and $\alpha=0$. The factor $\chi = \alpha k_B T$. Since μ is inversely proportional to F_c , the mobility decreases with increasing chiral angle. In Fig. 2, μ is given as a function of d for a zig-zag tube ($\phi_c=0$) at room temperature. For very small diameter tubes, μ is quite small but increases sharply with diameter as $d^{5/2}$. Here the band structure is parabolic and the nonparabolic term in square brackets above plays no role. As the diameter increases the band gap decreases and the low energy subband becomes more nonparabolic. The SWCNT is approaching graphene and the energy band structure dispersion becomes increasing more linear. As seen in Fig. 2, the α -dependent term in Eq. (3) acts to reduce μ . Once the tube diameter increases to $\sim 5\text{nm}$, the mobility varies only slowly with diameter.

Experimental measurements [1] for the low-field mobility of a $d=3.9\text{nm}$, 325 micron length semiconducting carbon nanotube are shown in Fig. 3. The tube chirality was unknown. The mobility is larger than $10^5 \text{ cm}^2/\text{Vs}$, agreeing with previous theoretical predictions [3, 4]. Alongside these measurements, the results of Eq. (3) are shown for the limiting cases of a zig-zag ($\phi_c=0^\circ$) and an armchair ($\phi_c \approx 30^\circ$) tube. Both the magnitude and the temperature

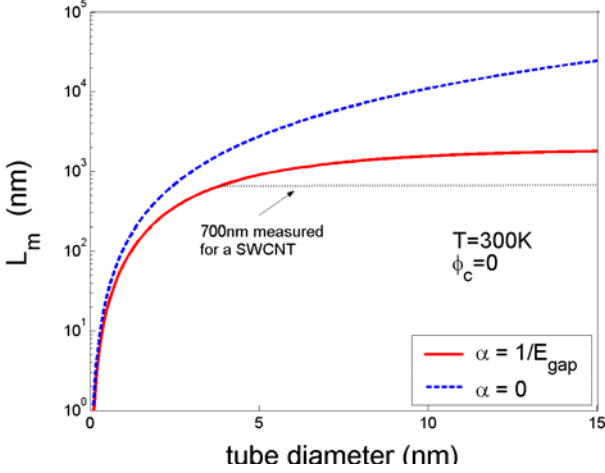


Figure 4: Phonon scattering mean free path vs. d

dependence of the model low-field mobility agree strongly with the experimental results.

The mean free path, corresponding to momentum relaxation at low fields can be derived from the product of the ensemble averaged relaxation time and the thermal velocity. The model predicts a mean free path of:

$$L_m = 109nm \cdot \frac{\tilde{d}^2}{F_c^2} \left[\frac{1 + \frac{1}{4}\chi - \frac{15}{32}\chi^2}{1 + 2\chi + 30\chi^2} \right]. \quad (4)$$

The mean free path as a function of tube diameter is given in Fig. 4. As found for the mobility, L_m increases with tube diameter and decreases with increasing ϕ_c when the tube diameter remains relatively small. Again this occurs since the effective mass is inversely proportional to d . As the $\alpha k_B T$ factor in L_m becomes important, the mean free path saturates. Results compare well with a measured mean free path of about 700nm [7] in a semiconducting nanotube.

III. CHARGE SCATTERING MOBILITY

Experiments indicate a large degree of charge trapping in SWCNT-FETs. It is believed that the large hysteresis typically observed in these devices results from the injection of carriers from the nanotube into the nearby oxide/SWCNT interface [1, 7]. A complete transport model should therefore also consider scattering with localized interface charges. Here the mobility in the presence of charges very close to the nanotube surface is presented.

We determine the matrix elements for the coulombic interaction of carriers with localized charges as:

$$\langle k' | H | k \rangle = \sum_j \frac{e^2 \Delta Q_j(\vec{x}_j)}{\pi L \bar{\epsilon}} e^{-iqz_j} \int_0^{2\pi} K_0(|q||\Delta\vec{r}_j|) d\theta. \quad (5)$$

In accord with the restriction of carriers to one subband at low fields, these elements describe intrasubband scattering only. Here e , L , $\hbar q$, and $\bar{\epsilon}$ are the electron charge, the tube length, the momentum transfer along z , and the static dielectric function respectively. The sum is over each charge scatter at position \vec{x}_j in 3-dimensional space. Following previous work for surface scattering in conventional devices [8], ΔQ_j is the fluctuation from the average charge on a cylindrical surface of radius r_j . The zero order modified Bessel function K_0 is evaluated at

$$|\Delta\vec{r}_j| = \sqrt{\frac{d^2}{4} + r_j^2 - r_j d \cos(\theta + \theta_j)}. \quad (6)$$

For a general distribution of charges ΔQ_j , Eq. (5) can be solved numerically. Here an analytical solution will be developed for the particular case of a random Poisson or Gaussian distribution of localized charges on a cylindrical surface very close to the SWCNT surface ($r_j \sim d/2$). This is a practical case since charge trapping likely occurs very close to the nanotube. An analytical relation can be developed in the limit of large tube length and small momentum transfer $qd \ll 1$. Such a small momentum transfer is likely since the density of carrier states varies as $\sqrt{1+2/qd}$ at the band edge. The static polarizability parallel to the tube axis [9], which is much larger than the perpendicular polarizability, is used to determine the SWCNT dielectric function

$$\bar{\epsilon} = \frac{\epsilon_{ox} + \epsilon_{SWCNT}}{2} = 2.5 + 5.5\tilde{d}. \quad (7)$$

If the band structure nonparabolicity (α) is ignored, the low-field mobility due to interface charge is

$$\mu_l = \frac{1.9e^{12}/V_S}{\bar{N}(d/2)} \cdot \left\{ \frac{\tilde{d}^{3/2} \sqrt{\tilde{T}} [2.5 + 5.5\tilde{d}]^2}{1 + 0.041 \ln^2(\tilde{T}\tilde{d}) - 0.39 \ln(\tilde{T}\tilde{d})} \right\} \quad (8)$$

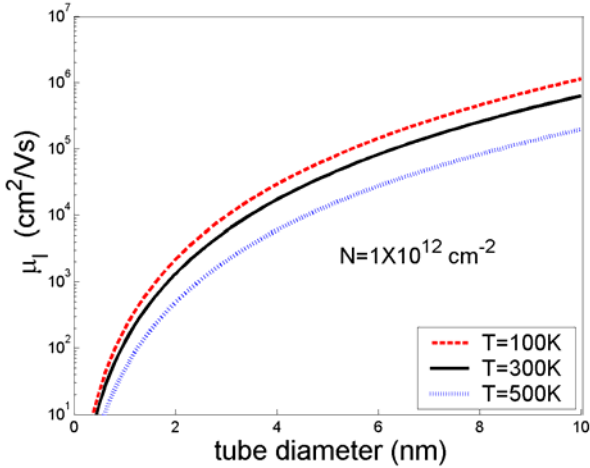


Figure 5: Interface charge mobility vs. d

where \bar{N} is the average 2D charge density of external charges on a cylinder or radius $d/2$. As seen in Fig. 5, the charge scattering mobility increases with tube diameter as was the case for μ_p . Here a charge density of $1 \times 10^{12} \text{ cm}^{-2}$ is considered. However; in contrast to μ_p , μ_c also increases with increasing temperature in Fig. 6, if \bar{N} remains fixed. If nonparabolic effects are included in the band structure, μ_I is likely to be reduced from the result of Eq. (8) for larger tube diameters.

IV. CONCLUSION

Models for low-field carrier transport in a single-walled carbon nanotube have been developed in the semiclassical regime. Results are appropriate for semiconducting tubes of varying diameter and chirality. Scattering from both acoustic phonons and charges at the nanotube/oxide interface are considered.

When phonon scattering dominates, the mobility is found to increase with tube diameter and lattice temperature according to $d^{5/2} \cdot T^{-1/2}$, when $d < \sim 5 \text{ nm}$. For larger diameters, the mobility increases more slowly with d due to nonparabolic band structure effects. The phonon scattering mobility model is found to agree well with experiments on a long, 3.9nm diameter nanotube, where very large mobilities exceeding $10^5 \text{ cm}^2/\text{Vs}$ have been observed [1].

The phonon scattering model predicts a mean free path increasing with tube diameter as d^2 , when $d < \sim 5 \text{ nm}$. For larger tubes, there is a temperature dependence and a slower increase with increasing diameter. Again, this is due to nonparabolic band structure effects. The transport modeling predicts a large mean free path of $\sim 1 \text{ micron}$ in larger tubes. This

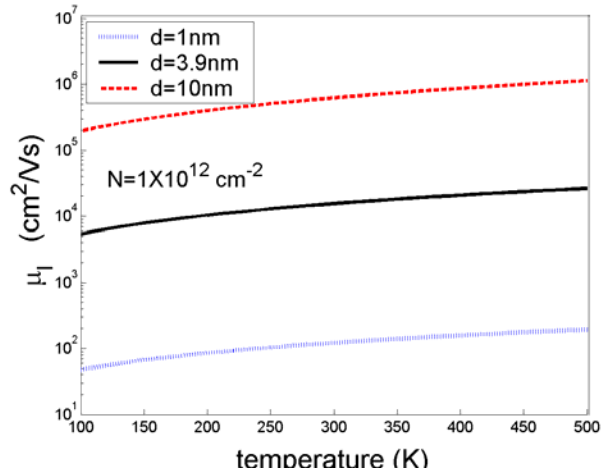


Figure 6: Interface charge mobility vs. T

agrees well with experiments [7].

When scattering from trapped charges or ionized impurities localized near the nanotube surface dominates transport, the interface mobility is found to be inversely proportional to the 2D interface charge concentration, as in conventional electronic devices [8]. As the tube diameter increases, μ_I increases as $d^{3/2}$. Nonparabolic band structure effects were not taken into account. The interface charge scattering mobility increases slowly with temperature. Values as large as $10^5 \text{ cm}^2/\text{Vs}$ are predicted for interface charge concentrations of 10^{12} cm^{-2} in large diameter tubes.

V. REFERENCES

- [1] T. Durkop, S. A. Getty, E. Cobas, and M. S. Fuhrer, *Nano Lett.* 4, p. 35 (2004).
- [2] A. Akturk, G. Pennington, and N. Goldsman, *IEEE Trans. Elect. Dev.* 52, p. 577 (2005).
- [3] G. Pennington and N. Goldsman, *Phys. Rev. B* 68, p. 45426 (2003).
- [4] G. Pennington and N. Goldsman, *SISPAD 2002*, p. 279 (2002).
- [5] L. Yang, M. P. Anantram, J. Han, and J. P. Lu, *Phys. Rev. B* 55, p. 6820 (1999).
- [6] H. Suzuura and T. Ando, *Phys Rev. B* 65, p. 235412 (2002).
- [7] T. Durkop, B. M. Kim, and M. S. Fuhrer, *J. Phys. B. Condens. Matt.* 16, p. R553 (2004)
- [8] C. T. Sah, T. H. Ning, and L. L. Tschopp, *Surface Sci.* 32, p. 561 (1972).
- [9] L. X. Benedict, S. G. Louie, and M. L. Cohen, *Phys. Rev. B* 52, p. 8541 (1995).